

# Shadow of a five-dimensional Reissner-Nordström Anti-de Sitter black hole

---

**Surajit Mandal**

*Department of Physics, Jadavpur University, Kolkata, West Bengal 700032, India*

*E-mail: [surajitmandalju@gmail.com](mailto:surajitmandalju@gmail.com)*

**ABSTRACT:** In this paper, we study the shadow cast by the five-dimensional charged Reissner-Nordström anti-de sitter black hole both for non-plasma and plasma medium. Using the symmetry directions and Hamilton-Jacobi equation we determine the null geodesic equations. With the help of null geodesics, we then evaluate the celestial coordinates  $(\alpha, \beta)$  and the radius of the black hole shadow  $R_s$ . We make a graphically analysis of black hole shadow in the celestial plane ( $\alpha, \beta$ -plane) and it is observed that shadow is a dark zone covered by a perfect circle. The effects of cosmological constant and charge of the black hole on the the shadow radius is studied in detail. In particular the size of the black hole shadow decreases for an increases in the values of charge of black hole. We then introduce a plasma medium in order to investigate the effect of plasma parameter on black hole shadow. We observe that shadow radius rises for an increase in plasma parameter with changing photon sphere radius. Finally, We study the energy emission rate of five-dimensional RN- $AdS_5$  black hole. We make a graphical analysis to check the dependency of energy emission rate on charge, cosmological constant and plasma parameter.

**KEYWORDS:** Black hole shadow; RN- $AdS_5$  black hole; Plasma medium; Energy emission rate.

---

## Contents

<b>1</b>	<b>Introduction</b>	<b>1</b>
<b>2</b>	<b>Five-dimensional Reissner-Nordström anti-de sitter black hole</b>	<b>3</b>
<b>3</b>	<b>Horizons</b>	<b>4</b>
<b>4</b>	<b>Particle motion for non-plasma medium</b>	<b>5</b>
<b>5</b>	<b>Constructing the black hole shadow</b>	<b>8</b>
<b>6</b>	<b>Effect of various parameters on shadow radius <math>R_s</math> in non-plasma medium</b>	<b>11</b>
<b>7</b>	<b>Shadow in presence of the plasma medium</b>	<b>11</b>
<b>8</b>	<b>Geodesics and the shadow</b>	<b>12</b>
<b>9</b>	<b>Dependence of shadow radius <math>R_s</math> on various parameters in plasma medium</b>	<b>17</b>
<b>10</b>	<b>Energy emission rate</b>	<b>19</b>
<b>11</b>	<b>Conclusion</b>	<b>19</b>

---

## 1 Introduction

The study of black hole is an old topic of physics from the discovery of Einstein's theory of general relativity (1915). Nowadays, it is sharply presumed that there exist black holes at the centres of most of the galaxies, for example, it is mostly accepted that supermassive black hole Sagittarius  $A^*$  or Sgr  $A^*$  is present in the galactic centre of Milky Way [1, 2] but recently the shadow of this supermassive black hole has been observed by EHT (Event Horizon Telescope) group [3]. Any objects moving near the black hole, has a intense gravitational attraction, within a critical radius must falls into the black hole. This is happen due to strong gravitational lensing. If an illuminated source of photon is present just behind the black hole, then photon particles can move in the vicinity of black holes

and can casts a shadow at a plane which can be visible by an viewer at infinity. The black hole shadow was first studied by Bardeen and can found in [4]. It has been demonstrated that the spherically symmetric (non-rotating, for example Schwarzschild black hole) black holes can cast a shadow of circular shape [5, 6], whereas the shadows of rotating (spinning) black holes are deformed from circular shape [7–12]. Nowadays, the study of shadow cast of black hole has becomes an active research field and received a momentous attention [13]. The shadow of Schwarzschild black hole has been studied in [14, 15]. The shadow of rotating black hole along with gravitomagnetic and electric charge can be found in [16]. The gravitational lensing and optical phenomena for the Janis-Newman-Winicour space-time [17], for the Kerr-Newman and for the Kerr-Newman-AdS spacetimes has studied in [18]. Peoples have investigated the shadow of other black holes, such as regular black holes [19–21], Kerr black holes [4], Kerr-Newman black holes [22], multi-black holes [23]. Shadow of black holes in extended Chern-Simons modified gravity and Einstein-Maxwell dilaton gravity can be found in [24] and shadow in Randall-Sundrum braneworld case was made in [25]. Recently, Ali Övgün and others have studied on black hole shadow of noncommutative black holes in Rastall gravity [44]. Testing of generalized Einstein-Cartan-Kibble-Sciama gravity using shadow Cast was made in [26]. Kimet Jusufi and others [27], have studied on shadows of 5D electrically charged Bardeen black holes. Shadow cast of rotating braneworld black holes with a cosmological constant was made in [28].

It is considered that black holes are highly gravitating compact and geometrical objects for study in four-dimensions and their existence in more than four-dimensions (especially in five-dimensions) has also included. Nowadays, black hole solutions in five-dimensional (5D) space-time have been the topic of intensive research, inspired by the ideas in braneworld cosmology, string theory and gauge/gravity duality. Various interesting and surprising results can be found [29]. The uniqueness theorems do not hold in more than four-dimensional space time because to the fact that there exist more degrees of freedom. The study of black-ring solutions in five-dimensions demonstrates that higher dimensional spacetime can approve the non-trivial topologies [30]. The structure of black hole shadows ( $4 + 1$ ) dimensions in the context of holography were investigated in [31]. Recently, the shadow of five-dimensional Gauss-Bonnet black hole has studied in [46]. Shadow of five-dimensional rotating Myers-Perry black hole [32] and rotating five-dimensional charged EMCS black holes [33] has also been studied. Such investigation indeed provide a good inspiration to study the black hole shadows for Reissner-Nordström Anti-de Sitter black hole in 5-dimensions. Reissner-Nordström Anti-de Sitter black hole solution in five-dimensions is a static, spherically symmetric exterior vacuum solution of the Einstein equations in RN-AdS<sub>5</sub> spacetime. Geodesic Motions near the five-dimensional Reissner-Nordström Anti-de Sitter black hole has studied in [34]. The goal of this paper is to investigate the shadow of charged RN-AdS<sub>5</sub> black hole in non-plasma medium as

well as in plasma medium.

This paper is presented in eleven parts. In section 2, we outline the five-dimensional RN-AdS<sub>5</sub> black hole solution. The horizon function and radius of the event horizon is calculated in section 3. In Section 4, using the Hamilton-Jacobi equation, we discuss the particle motion around the five-dimensional RN-AdS<sub>5</sub> black hole in non-plasma media and the shadow of this black hole for non-plasma medium has studied in section 5. We discuss the effect of various parameters on shadow radius for non-plasma medium in section 6. Similar to the non-plasma case, geodesics in presence of plasma medium are studied in section 7 and shadow for this plasma medium are presented in section 8. The behavior of shadow radius for various parameters in plasma medium are given in section 9. We discuss the energy emission rate of five-dimensional RN-AdS<sub>5</sub> black hole in Section 10. Finally, we conclude our results in Section 11.

## 2 Five-dimensional Reissner-Nordström anti-de sitter black hole

Consider a 5-dimensional spacetime with a negative cosmological constant. The field equations near the black hole are given by following equation [34]:

$$\bar{G}_{ab} = -\Lambda_{(5)}\bar{g}_{ab} + k_{(5)}^2\bar{T}_{ab} \quad (2.1)$$

where  $\bar{g}_{ab}$  is a 5-dimensional metric has a signature  $(-, +, +, +, +)$ ,  $\bar{G}_{ab}$  denotes the 5-dimensional Einstein tensor, the 5-dimensional energy-momentum tensor is represented by  $\bar{T}_{ab}$  and  $\Lambda_{(5)}$  represents the 5-dimensional cosmological constant. The constant  $k_{(5)}$  is defined as

$$k_{(5)}^2 = 8\pi G_{(5)} = M^{-3} \quad (2.2)$$

where  $G_{(5)}$  is the 5-dimensional Newton's constant and  $M$  is the 5-dimensional reduced Planck mass.

Now, we assume that the spacetime has a constant curvature  $\bar{K} = \frac{\alpha}{l^2}$ .  $\bar{K}$  is negative, i.e,  $\alpha = -1$  for AdS geometry while  $\bar{K}$  becomes positive and  $\alpha = 1$  for dS geometry. Consequently the radius of curvature of spacetime becomes

$$l = \sqrt{\frac{3\alpha}{\Lambda_{(5)}}} \quad (2.3)$$

and it gives the necessary length scale to have a horizon. For simplification purposes we shall avoid the subscript and will represent  $\Lambda_{(5)}$  by  $\Lambda$ . The exterior metric for the black hole field in five-dimension is given by

$$ds^2 = -f(r)dt^2 + \frac{dr^2}{f(r)} + r^2d\Omega_3^2 \quad (2.4)$$

where,

$$d\Omega_3^2 = d\theta^2 + \sin^2\theta(d\phi^2 + \sin^2\phi d\psi^2) \quad (2.5)$$

is the metric on unit 3-sphere. For this static, spherically symmetric exterior vacuum solution of the Einstein equations in RN-AdS<sub>5</sub>, the lapse function  $f(r)$  is defined as

$$f(r) = 1 - \left(\frac{2M}{r}\right)^2 + \left(\frac{q^2}{r^2}\right)^2 - \frac{\Lambda r^2}{6} \quad (2.6)$$

here,  $q$ ,  $M$  are the total charge and geometric mass of the black hole respectively.  $\Lambda$  is the cosmological constant.

### 3 Horizons

We can write the lapse function (2.6) as

$$f(r) = \frac{\Delta}{r^4} \quad (3.1)$$

here  $\Delta$  is the horizon function and depends only on the radial coordinate for a given  $M$ ,  $q$  and  $\Lambda$ . Now, the exterior metric (2.4) can be written as

$$ds^2 = -\frac{\Delta}{r^4}dt^2 + \frac{r^4}{\Delta}dr^2 + r^2(d\theta^2 + \sin^2\theta(d\phi^2 + \sin^2\phi d\psi^2)) \quad (3.2)$$

We know that the spacetime has an intrinsic singularity at  $r = 0$  and the nature of this singularity depends on the parameters such as cosmological constant  $\Lambda$  and charge  $q$ . Both this parameter can be chosen in such a manner that the spacetime may not have any spacelike naked singularity (Carrol 2004). The lapse function vanishes at the real, positive zeros of the horizon function, i.e,  $\Delta = 0$ , which gives

$$\Lambda r^6 - 6r^4 + 24M^2r^2 - 6q^4 = 0 \quad (3.3)$$

so the real, positive zeros of horizon function gives the position of the horizon, which indicating the coordinate singularities for this RN-AdS<sub>5</sub> black hole. Interestingly, among the six distinct roots of eq. (3.3), only one is real and positive, which provides us the radius of the event horizon of the RN-AdS<sub>5</sub> black hole. Numerical solution gives this positive root as :

$$r = \sqrt{\frac{2}{\Lambda} - \frac{242^{\frac{1}{3}}M^2}{\mathcal{P}} + \frac{122^{\frac{1}{3}}}{\Lambda\mathcal{P}} + \frac{\mathcal{P}}{32^{\frac{1}{3}}\Lambda}} \quad (3.4)$$

where

$$\mathcal{P} = \left(432 - 1296M^2\Lambda + 162q^4\Lambda^2 + \sqrt{4(-36 + 72M^2\Lambda)^3 + (432 - 1296M^2\Lambda + 162q^4\Lambda^2)^2}\right)^{\frac{1}{3}}$$

## 4 Particle motion for non-plasma medium

In order to find the shape of the shadow of RN- $AdS_5$  black hole we first need to determine the geodesic equations for the photons (null particle) around this black hole. The symmetry directions basically work on the issue of searching the geodesics by knowing the constants of motion related with the direction of symmetries. Let us take  $k^\mu$  as a vector along the direction of symmetry and  $u^\mu = \frac{dx^\mu}{d\lambda}$  as a tangent vector along a curve  $x^\mu = x^\mu(\lambda)$  with affine parameter  $\lambda$ . Now, with the help of the Killing equation, it can be shown that

$$k^\mu u_\mu = \text{constant} \quad (4.1)$$

if the trajectory  $x^\mu$  is a geodesic [35]. As the metric coefficients of (2.4) are independent of time, as a result there is a timelike Killing vector  $k^\mu = (1, 0, 0, 0, 0)$ . Then eq.(4.1) gives

$$k^0 u_0 = u_0 = -E. \quad (4.2)$$

The negative sign is chosen for convenience and has no other physical significance. This constant  $E$  is familiar as the relativistic energy per particle mass. Since the metric coefficients are also independent of  $\phi$  and  $\psi$ , so these coordinates are represents the other symmetry directions. Hence by choosing  $k^\mu = (0, 0, 0, 1, 0)$  for the  $\phi$  direction and  $k^\mu = (0, 0, 0, 0, 1)$  for the  $\psi$  direction, we get the following

$$k^3 u_3 = u_3 = L_\phi \quad (4.3)$$

$$k^4 u_4 = u_4 = L_\psi \quad (4.4)$$

The constants  $L_\phi$  and  $L_\psi$  are known as the angular momentum per particle mass. Now, the geodesic equations along these directions of symmetry can be calculated by using the above constants of motion. This can be written as follows :

$$\frac{dt}{d\lambda} = \frac{E}{f(r)} \quad (4.5)$$

$$\frac{d\phi}{d\lambda} = \frac{L_\phi}{r^2 \sin^2 \theta} \quad (4.6)$$

$$\frac{d\psi}{d\lambda} = \frac{L_\psi}{r^2 \cos^2 \theta} \quad (4.7)$$

The another two geodesic equations can be calculated with the help of the relativistic Hamilton-Jacobi equation

$$\frac{\partial S}{\partial \lambda} + \frac{1}{2} g^{\mu\sigma} \frac{\partial S}{\partial x^\mu} \frac{\partial S}{\partial x^\sigma} = 0. \quad (4.8)$$

Now, we assume an ansatz of the form [8] to solve the above Hamilton-Jacobi equation

$$S = \frac{1}{2} m_0^2 \lambda - Et + L_\phi \phi + L_\psi \psi + S_r(r) + S_\theta(\theta) \quad (4.9)$$

where  $S_r(r)$  and  $S_\theta(\theta)$ , respectively, are functions of  $r$  and  $\theta$ ,  $\lambda$  is the affine parameter and  $m_0$  denotes the rest mass of the test particle. Using eqs. (4.9) and (4.8), we obtain

$$\left(\frac{\partial S_\theta}{\partial \theta}\right)^2 + L_\phi^2 \cot^2 \theta + L_\psi^2 \tan^2 \theta + \frac{1}{2}m_0^2 - \frac{r^2 E^2}{f(r)} + r^2 f(r) \left(\frac{\partial S_r}{\partial r}\right)^2 + L_\phi^2 + L_\psi^2 = 0 \quad (4.10)$$

By rearranging (4.10),

$$\left(\frac{\partial S_\theta}{\partial \theta}\right)^2 + L_\phi^2 \cot^2 \theta + L_\psi^2 \tan^2 \theta + \frac{1}{2}m_0^2 = \frac{r^2 E^2}{f(r)} - r^2 f(r) \left(\frac{\partial S_r}{\partial r}\right)^2 - L_\phi^2 - L_\psi^2 = \mathcal{K} \quad (4.11)$$

where  $\mathcal{K}$  is the separation constant. As we know the relation  $p_\theta = \frac{\partial S}{\partial \theta} = \frac{\partial S_\theta}{\partial \theta}$ , so we obtain

$$\frac{\partial S_\theta}{\partial \theta} = r^2 \frac{\partial \theta}{\partial \lambda} \quad (4.12)$$

where we considered the condition  $p_\theta = \frac{\partial \mathcal{L}}{\partial \theta}$  and Lagrangian  $\mathcal{L}$  is given by

$$\mathcal{L} = \frac{1}{2} g_{\mu\nu} \dot{x}^\mu \dot{x}^\nu \quad (4.13)$$

here overdot represents the differentiation w.r.t affine parameter  $\lambda$ . Similarly, using the condition  $p_r = \frac{\partial S}{\partial r} = \frac{\partial S_r}{\partial r}$ , we can write

$$\frac{\partial S_r}{\partial r} = r^2 \frac{\partial r}{\partial \lambda} \quad (4.14)$$

In order to determine the null geodesics we set  $m_0 = 0$  and using the eqs. (4.12), (4.14) into eq.(4.11), we obtain

$$r^2 \left(\frac{dr}{d\lambda}\right) = \sqrt{\mathcal{R}(r)} \quad (4.15)$$

$$r^2 \left(\frac{d\theta}{d\lambda}\right) = \sqrt{\Theta(\theta)} \quad (4.16)$$

Where

$$\mathcal{R}(r) = r^4 E^2 - (L^2 + \mathcal{K})r^2 f(r) \quad (4.17)$$

$$\Theta(\theta) = \kappa - L_\phi^2 \cot^2 \theta - L_\psi^2 \tan^2 \theta \quad (4.18)$$

here  $\mathcal{K}$  is known as the Carter's constant. The above eqs. (4.15) and (4.16) are the geodesic equations along  $r$  and  $\theta$  respectively.

Using eq.(4.15), we can arrive at the equation in the following familiar form :

$$\left(\frac{dr}{d\lambda}\right)^2 + V_{eff}(r) = 0 \quad (4.19)$$

where  $V_{eff}$  is the effective potential, given by

$$V_{eff}(r) = \frac{f(r)}{r^2} (\kappa + L^2) - E^2$$

$$L^2 \equiv L_\phi^2 + L_\psi^2 \quad (4.20)$$

In order to determine the unstable circular orbits we consider the following conditions :

$$V_{eff}(r)|_{r=r_p} = 0, \quad \frac{\partial V_{eff}(r)}{\partial r} \Big|_{r=r_p} = 0 \quad (4.21)$$

Now,  $V_{eff}(r)$  will be a maxima at  $r = r_p$  when

$$\frac{\partial^2 V_{eff}(r)}{\partial r^2} \Big|_{r=r_p} < 0 \quad (4.22)$$

where  $r_p$  is the radius of the photon sphere. Now using eq. (4.20), the first condition of (4.21) leads to

$$\frac{r_p^2}{f(r_p)} = \eta + (\xi_1^2 + \xi_2^2) \equiv \eta + \xi^2, \quad \xi^2 \equiv \xi_1^2 + \xi_2^2 \quad (4.23)$$

where we have considered the Chandrasekhar constants  $\eta, \xi_1$  and  $\xi_2$  [8] have the form :

$$\eta = \frac{\mathcal{K}}{E^2}, \quad \xi_1 = \frac{L_\phi}{E}, \quad \xi_2 = \frac{L_\psi}{E}. \quad (4.24)$$

Now, the boundary condition  $\frac{\partial V_{eff}(r)}{\partial r} \Big|_{r=r_p} = 0$  gives to

$$r f'(r) \Big|_{r=r_p} = 2 f(r) \Big|_{r=r_p} \quad (4.25)$$

Now, the first derivative  $f'(r)$  is given by using the metric function  $f(r)$  from eq.(2.6) and obtained as

$$f'(r) = \frac{8M^2}{r^3} - \frac{4q^4}{r^5} - \frac{1}{3}\Lambda r \quad (4.26)$$

We get from eq. (4.25)

$$r_p^4 - 8M^2 r_p^2 + 3q^4 = 0 \quad (4.27)$$

The solution of this equation gives the radius of the photon sphere as

$$r_p = \sqrt{\frac{8M^2 + \sqrt{64M^4 - 12q^4}}{2}} \quad (4.28)$$

## 5 Constructing the black hole shadow

To get the shadow of the RN-AdS<sub>5</sub> black hole, we will introduce the celestial coordinates which are shown schematically in figure 1 . For (4 + 1)- dimensions, the celestial coordinates becomes [36]

$$\begin{aligned}\alpha &= \lim_{r \rightarrow \infty} - \left( r^2 \sin \theta \frac{d\phi}{dr} + r^2 \cos \theta \frac{d\psi}{dr} \right) \\ \beta &= \lim_{r \rightarrow \infty} r^2 \sin \theta \frac{d\theta}{dr}\end{aligned}\quad (5.1)$$

where celestial coordinates  $\alpha$  and  $\beta$  represents the apparent perpendicular distance of

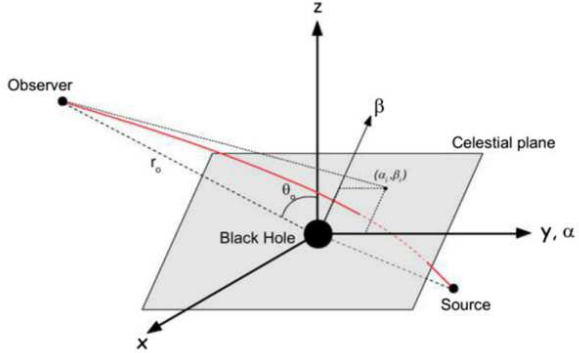


**Figure 1.** Schematic diagram for celestial coordinates [37].

the shadow as observe from the z-axis (axis of symmetry) and the apparent perpendicular distance of the shadow as observe from it's projection on the equatorial plane respectively,  $r_0$  denotes the distance of the viewer from the black hole and  $\theta$  is the inclination angle, is the angle between the observer's line of sight and the rotation axis of the black hole. Recalling the geodesic equations derived in eqs. (4.5) and (4.15), we get the values of  $\frac{d\phi}{dr}$ ,  $\frac{d\psi}{dr}$  and  $\frac{d\theta}{dr}$  as following :

$$\frac{d\phi}{dr} = \frac{L_\phi \csc^2 \theta}{r^2 \sqrt{E^2 - \frac{f(r)}{r^2} (\mathcal{K} + L_\phi^2 + L_\psi^2)}} \quad (5.2)$$

$$\frac{d\psi}{dr} = \frac{L_\phi \sec^2 \theta}{r^2 \sqrt{E^2 - \frac{f(r)}{r^2} (\mathcal{K} + L_\phi^2 + L_\psi^2)}} \quad (5.3)$$

$$\frac{d\theta}{dr} = \frac{1}{r^2} \sqrt{\frac{\mathcal{K} - L_\phi^2 \cot^2 \theta - L_\psi^2 \tan^2 \theta}{E^2 - \frac{f(r)}{r^2} (\mathcal{K} + L_\phi^2 + L_\psi^2)}} \quad (5.4)$$

Plugging the above equations into the eq. (5.1), we get

$$\alpha = -\frac{(\xi_1 \csc \theta + \xi_2 \sec \theta)}{\sqrt{1 + (\eta + \xi_1^2 + \xi_2^2)\Lambda}} \quad (5.5)$$

$$\beta = \pm \sqrt{\frac{(\eta - \xi_1^2 \cot^2 \theta - \xi_2^2 \tan^2 \theta)}{1 + (\eta + \xi_1^2 + \xi_2^2)\Lambda}} \quad (5.6)$$

Let us consider two different values of  $\theta$ , they are  $\theta = 0, \frac{\pi}{2}$ . If  $\theta = \frac{\pi}{2}$  then  $L_\psi = 0$  and as a result  $\xi_1 \equiv \xi$ . On the other hand, when  $\theta = 0$ ,  $L_\phi = 0$  which indicates  $\xi_2 \equiv \xi$ . Taking into account both the cases together the above celestial coordinates takes the form :

$$\alpha = -\frac{\xi}{\sqrt{1 + (\eta + \xi^2)\Lambda}} \quad (5.7)$$

$$\beta = \pm \sqrt{\frac{\eta}{1 + (\eta + \xi^2)\Lambda}} \quad (5.8)$$

Combining the eqs. (5.7) and (5.8), we arrive at the equation of a circle of radius  $R_s$  in the celestial plane ( $\alpha - \beta$  plane),

$$\alpha^2 + \beta^2 = \frac{\eta + \xi^2}{1 + (\eta + \xi^2)\Lambda} \equiv R_s^2 \quad (5.9)$$

here  $R_s$  is the radius of the shadow for non-plasma medium.

We have shown the computed values of RN-AdS<sub>5</sub> black hole shadow radius  $R_s$  and photon radius  $r_p$  for different values of charge  $q$  and cosmological constant  $\Lambda$  in table 1 and 2.

q	$r_p$	$\Lambda$	$R_s$
0.1	2.82842		3.76177
0.3	2.82789		3.76135
0.5	2.82427	0.0098	3.75851
0.7	2.81228		3.74914

**Table 1.** Radius of the black hole shadow  $R_s$  for varying  $q$  with  $\Lambda = 0.0098$ .

In figure 2, the variation of the black hole shadow in celestial plane ( $\alpha, \beta$ ) for different values of the charge  $q$  and cosmological constant  $\Lambda = 0.0098, 0.018$  is shown graphically. We

q	$r_p$	$\Lambda$	$R_s$
0.1	2.82842		3.5921
0.3	2.82789		3.59174
0.5	2.82427	0.018	3.58927
0.7	2.81228		3.5811

**Table 2.** Radius of the black hole shadow  $R_s$  for varying  $q$  with  $\Lambda = 0.018$ .

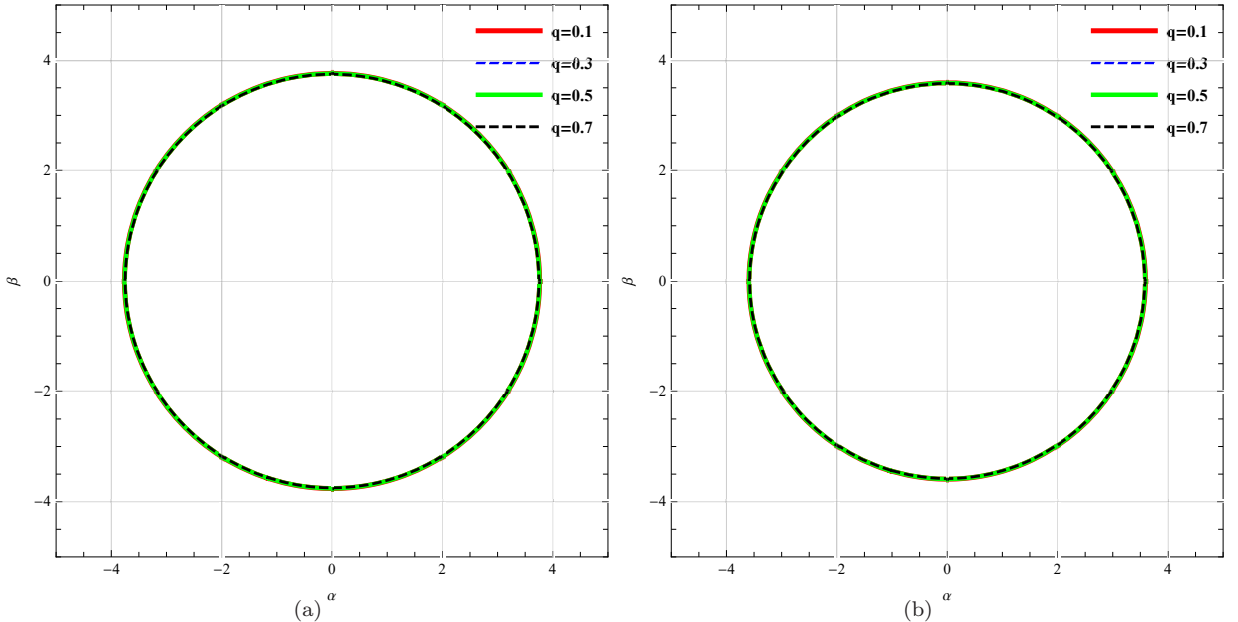


**Figure 2.** In (2(a)), black hole shadow in the celestial plane ( $\alpha$ - $\beta$  plane) for different values of  $q$  with cosmological constant  $\Lambda = 0.0098$ . In (2(b)), black hole shadow in the celestial plane ( $\alpha$ - $\beta$  plane) for different values of  $q$  with cosmological constant  $\Lambda = 0.018$ . Here,  $M = 1$

observe from the plots that the size of the black hole shadow decreases for an increase in the value of the charge parameter  $q$ . However, for an increase in the value of cosmological constant parameter the size of the radius of shadow also decreases.

## 6 Effect of various parameters on shadow radius $R_s$ in non-plasma medium

In this section, we study the effect of various parameter on shadow radius  $R_s$  for non-plasma medium. Now, the expression of the shadow radius in non-plasma medium read

$$R_s = \sqrt{\frac{\eta + \xi^2}{1 + (\eta + \xi^2)\Lambda}} = \sqrt{\frac{\frac{r_p^2}{f(r_p)}}{1 + \Lambda \frac{r_p^2}{f(r_p)}}} \quad (6.1)$$

here we have used eq. (4.23) in the second equality. It is notified that shadow radius depends on the parameters like cosmological constant  $\Lambda$ , charge  $q$  and mass  $M$  of the black hole.

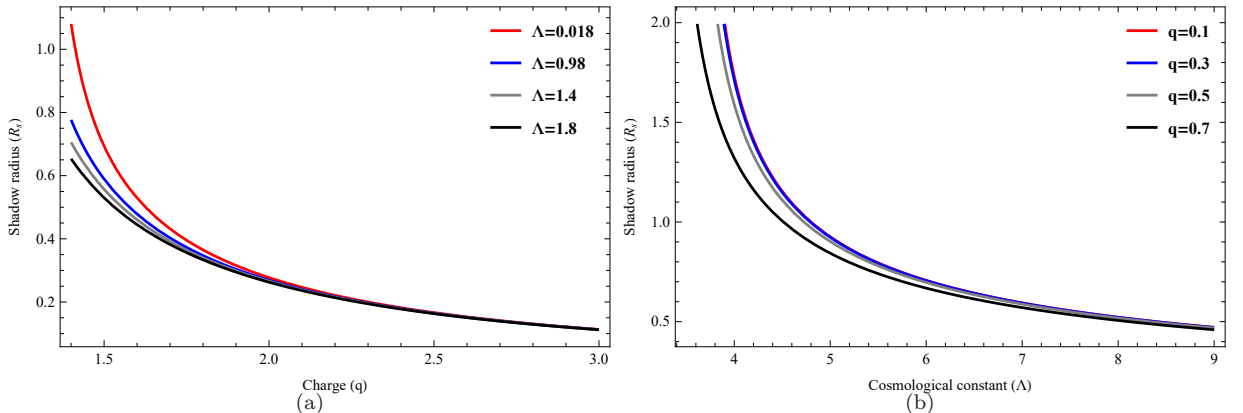


**Figure 3.** In 3(a), variation of the radius of the black hole shadow  $R_s$  with charge  $q$  for changing cosmological constant  $\Lambda$ . In 3(b), variation of the radius of the black hole shadow  $R_s$  with cosmological constant  $\Lambda$  for changing charge  $q$ . Here,  $M = 1$

Figure 3 depicts how shadow radius for non-plasma medium depends on parameter like charge  $q$  and cosmological constant  $\Lambda$ . In 3(a), shadow radius is a decreasing function of charge for fixed photon sphere radius. we see that for larger  $\Lambda$  values shadow radius curve decreases sharply. However, in plot 3(b), shadow radius is a decreasing function of  $\Lambda$  and here shadow radius curve decreases for increasing charge parameter  $q$ .

## 7 Shadow in presence of the plasma medium

In this section, we will study the effects of a plasma medium on the shadow of RN- $AdS_5$  black hole. Generally a black hole is surrounded by a material media which affects on

the motion of null like particles (photons) passing through it. The refractive index for the plasma media is given by  $n = n(x^i, \omega)$ , where  $\omega$  is the photon frequency measured by an viewer moving with a velocity  $u^\mu$ . The Hamiltonian is now modified by this plasma background. Due to this medium there appears an additional terms in the equations of geodesic motion and hence the trajectories of photons get modified and illustrates explicitly frequency dependent nature. Due to this plasma effect, effective energy of particle also get modified and given by  $E = \hbar\omega = -p_\alpha u^\alpha$ . The relationship between the refractive index and the 4-momentum of the photon is given by [38]

$$n^2 = 1 + \frac{p_\alpha u^\alpha}{(p_\mu u^\mu)^2}. \quad (7.1)$$

Now, both the refractive index ( $n$ ) and plasma frequency ( $\omega_p$ ) have a relation [39]

$$n = \sqrt{1 - \left(\frac{\omega_p}{\omega}\right)^2} \quad (7.2)$$

where  $\omega_p$  is defined by

$$\omega_p = \frac{4\pi e^2 N(r)}{m_e} \quad (7.3)$$

Here,  $e, N(r)$  and  $m_e$  are, respectively, the charge, number density and electron mass in the plasma medium. The physical form of  $N(r)$  is considered to be  $\frac{N_0}{r^i}$ , as defined in [38, 39]. Replacing the form of  $N(r)$  in the plasma frequency  $\omega_p$  and from eq.(7.2) we have a relation

$$\left(\frac{\omega_p}{\omega}\right)^2 = \frac{k}{r^i}, k \geq 0. \quad (7.4)$$

The power  $i$  identifies various properties of the plasma medium but we shall take  $i = 1$  which reflects the minimum dependency on  $r$  [39, 40]. Consequently, the expression for refractive index  $n$  with which we will deal in the rest of the calculation becomes

$$n = \sqrt{1 - \frac{k}{r}} \quad (7.5)$$

The modified expression of the Hamilton-Jacobi equation reads [38]

$$\left(\frac{\partial S}{\partial \lambda}\right) + \frac{1}{2} \left[ g^{\mu\sigma} \frac{\partial S}{\partial x^\mu} \frac{\partial S}{\partial x^\sigma} - (n^2 - 1) \left(\frac{\partial S}{\partial t} \sqrt{-g^{tt}}\right)^2 \right] = 0. \quad (7.6)$$

## 8 Geodesics and the shadow

In order to study the effect of a plasma medium on black hole shadow, we need to take into account the new set of celestial coordinates. We start the analysis by considering the modified geodesic equations. Now, for plasma medium the set of null geodesics reads

$$\frac{dt}{d\lambda} = \frac{n^2 E}{f(r)} \quad (8.1)$$

$$\frac{d\phi}{d\lambda} = \frac{L_\phi}{r^2 \sin^2 \theta} \quad (8.2)$$

$$\frac{d\psi}{d\lambda} = \frac{L_\psi}{r^2 \cos^2 \theta} \quad (8.3)$$

$$r^2 \left( \frac{dr}{d\lambda} \right) = \pm \sqrt{\mathcal{R}_{pl}(r)} \quad (8.4)$$

$$r^2 \left( \frac{d\theta}{d\lambda} \right) = \pm \sqrt{\Theta_{pl}(\theta)} \quad (8.5)$$

where

$$\mathcal{R}_{pl}(r) = n^2 r^4 E^2 - (L^2 + \mathcal{K}) r^2 f(r) \quad (8.6)$$

$$\Theta_{pl}(\theta) = \mathcal{K} - L_\phi^2 \cot^2 \theta - L_\psi^2 \tan^2 \theta \quad (8.7)$$

For this modified geodesic equations, we can follow the method studied in the previous section and also use the Hamilton-Jacobi equation (7.6). The effective radial potential in presence of the plasma background reads

$$V_{eff}^{pl}(r) = \frac{f(r)}{r^2} (\mathcal{K} + L^2) - n^2 E^2. \quad (8.8)$$

For the unstable circular orbits we can follow :

$$V_{eff}^{pl}(r) \Big|_{r=r_p^{(pl)}} = 0, \quad \frac{\partial V_{eff}^{pl}(r)}{\partial r} \Big|_{r=r_p^{(pl)}} = 0 \quad (8.9)$$

For maximizing condition of  $V_{eff}^{pl}(r)$ ,

$$\frac{\partial^2 V_{eff}^{pl}(r)}{\partial r^2} \Big|_{r=r_p^{(pl)}} < 0. \quad (8.10)$$

The first condition in eq. (8.9) leads to

$$\eta + \xi^2 = \frac{n^2(r) r^2}{f(r)} \Big|_{r=r_p^{(pl)}} \quad (8.11)$$

and the second condition gives

$$\left( n(r) r f'(r) - 2n(r) f(r) - 2n'(r) r f(r) \right) \Big|_{r=r_p^{(pl)}} = 0 \quad (8.12)$$

Now recalling  $f(r)$  and  $f'(r)$  from eqs. (2.6) and (4.26) along with  $n'(r) = \frac{k}{2r^2 \sqrt{1-\frac{k}{r}}}$  (from eq. (7.5)) in eq.(8.12), we obtain the equation for the radius of the photon sphere as

$$\begin{aligned} 0 = & \sqrt{1 - \frac{k}{r_p}} \left( \frac{8M^2}{r_p^2} - \frac{4q^4}{r_p^4} - \frac{1}{3} \Lambda r_p^2 \right) - 2 \sqrt{1 - \frac{k}{r_p}} \left( 1 - \left( \frac{2M}{r_p} \right)^2 + \left( \frac{q^2}{r_p^2} \right)^2 - \frac{\Lambda r_p^2}{6} \right) \\ & - \frac{k}{r_p \sqrt{1 - \frac{k}{r_p}}} \left( 1 - \left( \frac{2M}{r_p} \right)^2 + \left( \frac{q^2}{r_p^2} \right)^2 - \frac{\Lambda r_p^2}{6} \right) \end{aligned} \quad (8.13)$$

Here, it is not possible to get an exact solution of eq. (8.13). So we can proceed to solve this equation numerically. An extra parameter  $k$  arises in eq. (8.13) due to the effect of plasma medium. Let us consider two values of  $k$  which are 0.2 and 0.4 and for this values we obtain the radius of photon sphere  $r_p$  by solving eq. (8.13) numerically. As like before, we obtain an expressions for  $\frac{d\phi}{dr}$ ,  $\frac{d\psi}{dr}$  and  $\frac{d\theta}{dr}$  for the plasma medium, which will be used to calculate the celestial coordinates  $(\alpha, \beta)$  for this medium. The modified expressions are

$$\frac{d\phi}{dr} = \frac{L_\phi \csc^2 \theta}{r^2 \sqrt{n^2 E^2 - \frac{f(r)}{r^2} (\mathcal{K} + L_\phi^2 + L_\psi^2)}} \quad (8.14)$$

$$\frac{d\psi}{dr} = \frac{L_\phi \sec^2 \theta}{r^2 \sqrt{n^2 E^2 - \frac{f(r)}{r^2} (\mathcal{K} + L_\phi^2 + L_\psi^2)}} \quad (8.15)$$

$$\frac{d\theta}{dr} = \frac{1}{r^2} \sqrt{\frac{\mathcal{K} - L_\phi^2 \cot^2 \theta - L_\psi^2 \tan^2 \theta}{n^2 E^2 - \frac{f(r)}{r^2} (\mathcal{K} + L_\phi^2 + L_\psi^2)}} \quad (8.16)$$

Plugging the above equations into the expressions of the celestial coordinates  $(\alpha, \beta)$  defined in (5.1), we get

$$\alpha = -\frac{(\xi_1 \csc \theta + \xi_2 \sec \theta)}{\sqrt{1 + (\eta + \xi_1^2 + \xi_2^2) \Lambda}} \quad (8.17)$$

$$\beta = \pm \sqrt{\frac{(\eta - \xi_1^2 \cot^2 \theta - \xi_2^2 \tan^2 \theta)}{1 + (\eta + \xi_1^2 + \xi_2^2) \Lambda}} \quad (8.18)$$

Similar to the non-plasma medium, we shall take two different values of  $\theta$ , i.e,  $\frac{\pi}{2}$  and  $0$ . For both cases, the celestial coordinates becomes

$$\alpha = -\frac{\xi}{\sqrt{1 + (\eta + \xi^2) \Lambda}} \quad (8.19)$$

$$\beta = \pm \sqrt{\frac{\eta}{1 + (\eta + \xi^2) \Lambda}} \quad (8.20)$$

Taking into account the celestial coordinates from eqs.(8.19) and (8.20) and using eq. (8.11), we get

$$\alpha^2 + \beta^2 = \frac{\eta + \xi^2}{1 + (\eta + \xi^2) \Lambda} = \frac{\frac{n^2 r_p^2}{f(r_p)}}{1 + \Lambda \frac{n^2 r_p^2}{f(r_p)}} \equiv R_s^2 \quad (8.21)$$

where  $R_s$  denotes the radius of the black hole shadow for the plasma medium.

Tables 3, 4, 5 and 6 illustrates the computed values of the RN- $AdS_5$  black hole shadow radius  $R_s$  and photon radius  $r_p$  for different values of charge  $q$  of the black hole and cosmological constant  $\Lambda$  in presence of the plasma medium.

q	$r_p$	$R_s$
0.1	2.16013	4.54487
0.3	2.15914	4.54799
0.5	2.15233	4.57085
0.7	2.12942	4.65152

**Table 3.** Radius of the black hole shadow  $R_s$  for varying  $q$  with  $k = 0.2$ ,  $\Lambda = 0.018$  and  $M = 1$ .

q	$r_p$	$R_s$
0.1	2.15985	4.89338
0.3	2.15885	4.90248
0.5	2.15205	4.93012
0.7	2.12914	5.03282

**Table 4.** Radius of the black hole shadow  $R_s$  for varying  $q$  with  $k = 0.2$ ,  $\Lambda = 0.0098$  and  $M = 1$ .

q	$r_p$	$R_s$
0.1	2.11695	4.77485
0.3	2.11592	4.78018
0.5	2.10887	4.81765
0.7	2.08512	4.95895

**Table 5.** Radius of the black hole shadow  $R_s$  for changing  $q$  with  $k = 0.4$ ,  $\Lambda = 0.018$  and  $M = 1$ .

In celestial plane  $(\alpha, \beta)$ , the dependence of the black hole shadow on charge  $q$  and plasma parameter  $k$  with cosmological constant  $\Lambda = 0.018$  for plasma medium is depicted in figure 4. We see that shadow radius increases for an increase in plasma parameter  $k$  with different photon sphere radius. It is also observed from the plots that the size of the black hole shadow increases for an increase in the value of the charge parameter  $q$ .

$q$	$r_p$	$R_s$
0.1	2.11636	5.18284
0.3	2.11533	5.18966
0.5	2.10828	5.23775
0.7	2.08453	5.421

**Table 6.** Radius of the black hole shadow  $R_s$  for varying  $q$  with  $k = 0.4$ ,  $\Lambda = 0.0098$  and  $M = 1$ .

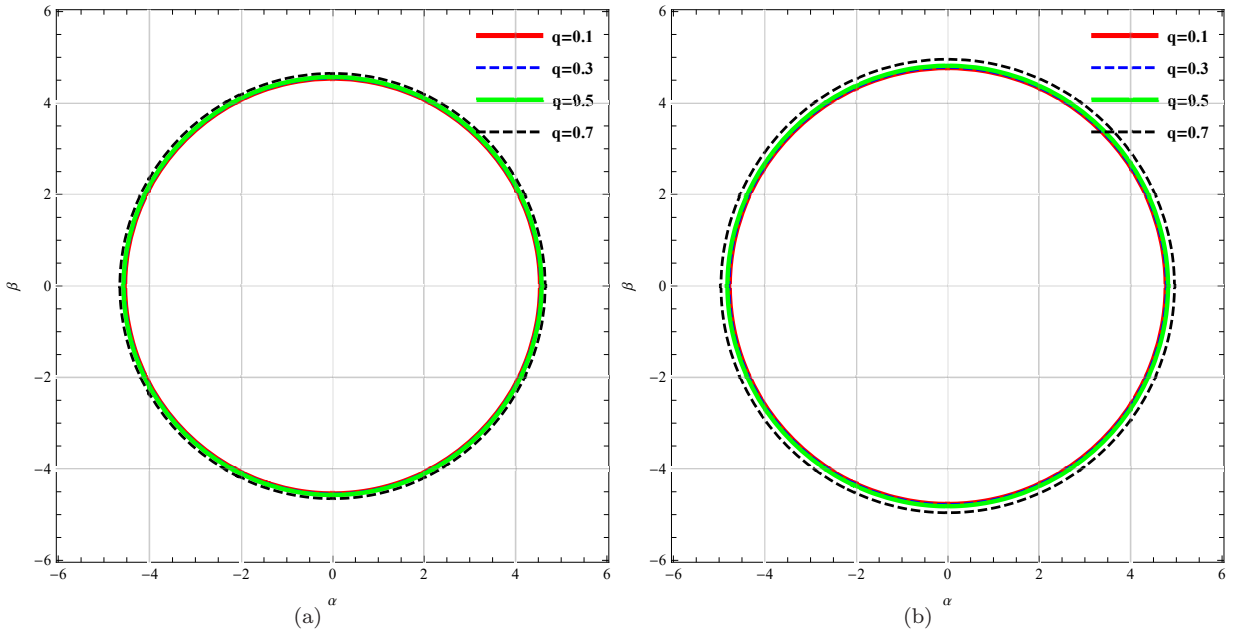


**Figure 4.** In (4(a)), black hole shadow in the celestial plane ( $\alpha$ - $\beta$  plane) for different values of  $q$  with  $k = 0.2$ . In (4(b)), black hole shadow in the celestial plane ( $\alpha$ - $\beta$  plane) for different values of  $q$  with  $k = 0.4$ . Here,  $\Lambda = 0.018$  and  $M = 1$

Figure 5 depicts the dependence of the black hole shadow on charge  $q$  and plasma parameter  $k$  with cosmological constant  $\Lambda = 0.0098$  in celestial plane ( $\alpha, \beta$ ) for plasma medium. We see that shadow radius enlarges for an increase in plasma parameter  $k$  with changing photon sphere radius. It is also evident from the plots that the size of the black hole shadow rises for an increase in the value of the charge parameter  $q$ .

In the next section we will discuss the dependence of the shadow radius with  $q$  and  $\Lambda$  for two different values of  $k$ .

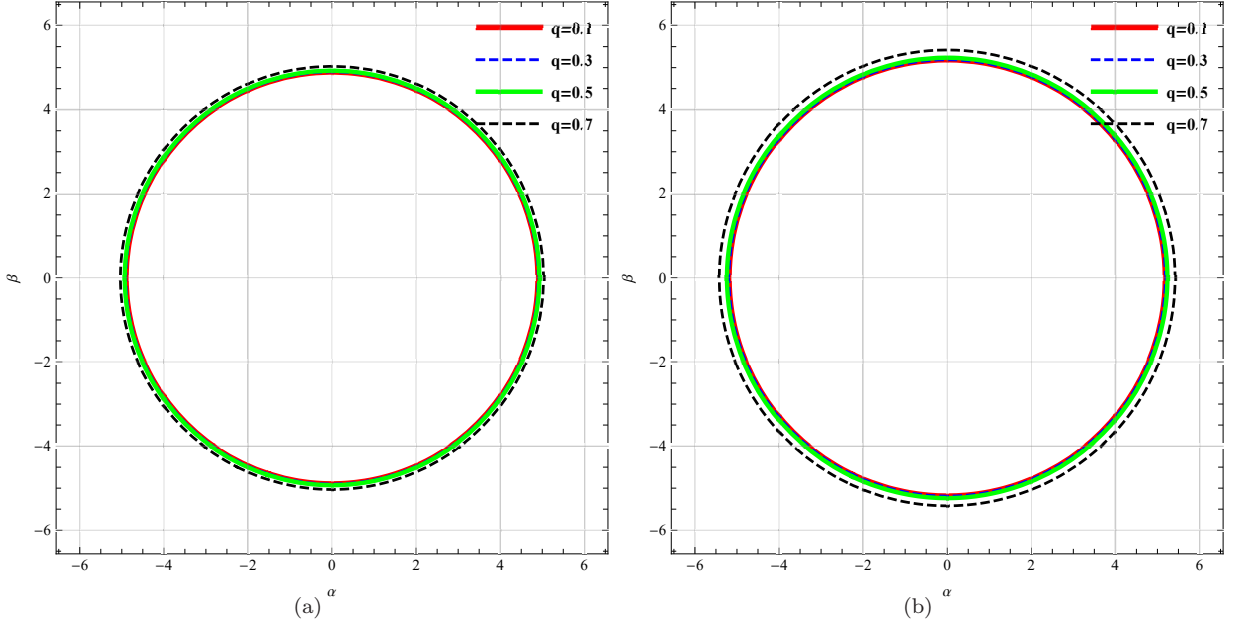


**Figure 5.** In 5(a), black hole shadow in the celestial plane ( $\alpha$ - $\beta$  plane) for different values of  $q$  with  $k = 0.2$ . In (5(b)), black hole shadow in the celestial plane ( $\alpha$ - $\beta$  plane) for different values of  $q$  with  $k = 0.4$ . Here,  $\Lambda = 0.0098$  and  $M = 1$

## 9 Dependence of shadow radius $R_s$ on various parameters in plasma medium

In this section, we will study the effect of various parameter on shadow radius  $R_s$  for plasma media. Now, the expression of the shadow radius  $R_s$  in the presence of the plasma medium reads

$$R_s^2 = \sqrt{\frac{\frac{n^2 r_p^2}{f(r_p)}}{1 + \Lambda \frac{n^2 r_p^2}{f(r_p)}}} \quad (9.1)$$

It is evident that shadow radius  $R_s$  depends on the parameters such as cosmological constant  $\Lambda$ , charge  $q$  and the plasma parameter  $k$ .

Figure 6 depicts how shadow radius for plasma medium depends on parameter like charge  $q$  and cosmological constant  $\Lambda$  for  $k = 0.2$ . In 6(a), shadow radius is a decreasing function of charge for fixed values of photon sphere radius. we see that for larger  $\Lambda$  values shadow radius curve decreases sharply. However, in plot 6(b), shadow radius is a decreasing function of  $\Lambda$  for fixed photon sphere radius. Moreover, the shadow radius curve decreases for increasing charge parameter  $q$ .

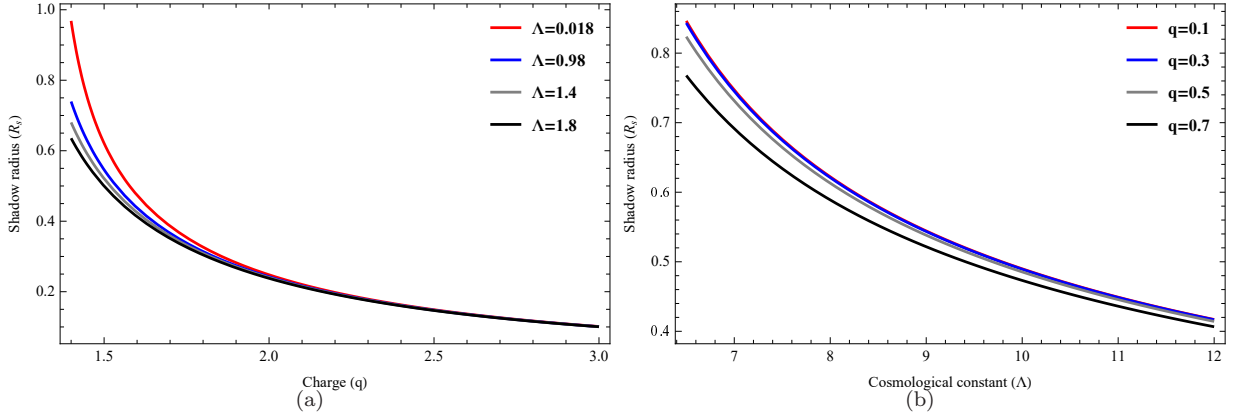


**Figure 6.** In 6(a), variation of the radius of the black hole shadow  $R_s$  with charge  $q$  for changing cosmological constant  $\Lambda$ . In 6(b), variation of the radius of the black hole shadow  $R_s$  with cosmological constant  $\Lambda$  for changing charge  $q$ . Here,  $k = 0.2$  and  $M = 1$

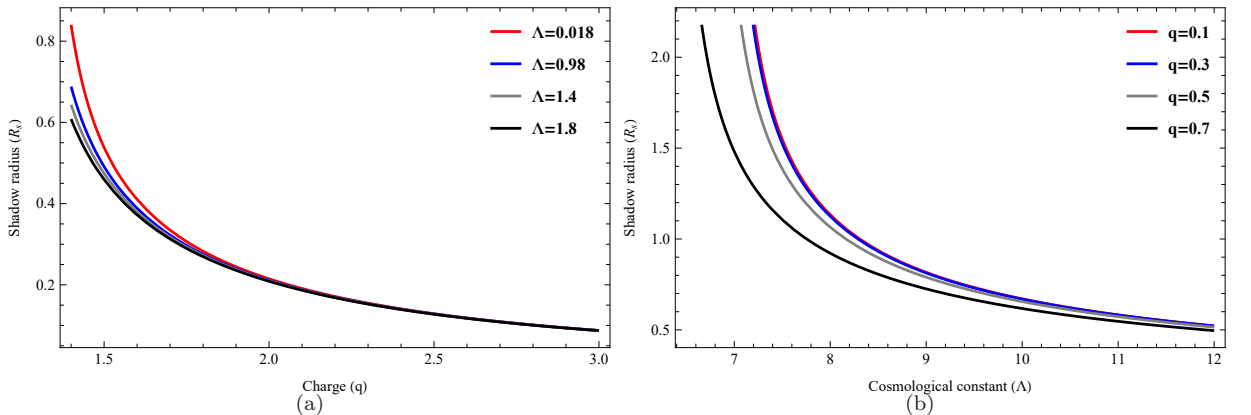


**Figure 7.** In 7(a), variation of the radius of the black hole shadow  $R_s$  with charge  $q$  for changing cosmological constant  $\Lambda$ . In 7(b), variation of the radius of the black hole shadow  $R_s$  with cosmological constant  $\Lambda$  for changing charge  $q$ . Here,  $k = 0.4$  and  $M = 1$

Figure 7 depicts how shadow radius for plasma medium depends on parameter like charge  $q$  and cosmological constant  $\Lambda$  with  $k = 0.4$ . In 7(a), shadow radius is a decreasing function of  $q$  for fixed values of photon sphere radius. we see that shadow radius curve decreases sharply for larger  $\Lambda$  values. However, in plot 7(b), shadow radius is a decreasing function of  $\Lambda$  for fixed photon sphere radius. Moreover, the shadow radius curve falls for increasing charge parameter  $q$ .

Figures 6 and 7 shows that, for a fixed photon sphere radius, shadow radius  $R_s$  reduces with an increase in plasma parameter  $k$ .

## 10 Energy emission rate

In this section, we study the energy emission rate of five-dimensional Reissner-Nordström anti-de sitter black hole. The expression of energy emission rate reads [41–44]

$$\frac{d^2Z(\omega)}{d\omega dt} = \frac{2\pi^2\sigma_{lim}}{\exp\left(\frac{\omega}{T_H}\right) - 1}\omega^3 \quad (10.1)$$

where  $Z(\omega)$ ,  $T_H$  and  $\omega$  denotes the energy, Hawking temperature and frequency corresponding to the black hole. The Hawking temperature can be calculated as [45]

$$T_H = \left. \frac{f'(r)}{4\pi} \right|_{r=r_+} = \frac{2M^2}{\pi r_+^3} - \frac{q^4}{\pi r_+^5} - \frac{\Lambda r_+}{12\pi} \quad (10.2)$$

here  $r_+$  is the event horizon radius of RN-AdS<sub>5</sub> black hole.

For five-dimensional black hole  $\sigma_{lim}$  reads [46–48]

$$\sigma_{lim} = \frac{4\pi R_s^3}{3} \quad (10.3)$$

Therefore, the energy emission rate in five-dimensions becomes

$$\frac{d^2Z(\omega)}{d\omega dt} = \frac{8\pi^3 R_s^3}{3 \left( \exp\left(\frac{\omega}{T_H}\right) - 1 \right)} \omega^3 \quad (10.4)$$

Figure 8 depicts the variation of energy emission rate  $\frac{d^2Z(\omega)}{d\omega dt}$  with frequency  $\omega$  for changing charge  $q$ , changing photon sphere radius and for plasma parameter  $k = 0, 0.2$ . We see that energy emmision rate decreases for increases in charge for non-plasma meduium and energy emission rate increases for increases in charge for plasma meduium. Plasma parameter  $k$  increases the energy emission rate. However, the variation of energy emission rate  $\frac{d^2Z(\omega)}{d\omega dt}$  with frequency  $\omega$  for changing charge  $q$ , changing photon sphere radius and for plasma parameter  $k = 0.4$  has shown in figure 9. Here it is more clear that the energy emission rate increases for increases in the values of charge.

## 11 Conclusion

We now summarize our results here. In this paper, we investigate the shadow of RN-AdS<sub>5</sub> black holes for an infinitely distant observer. We first evaluate the null geodesic equations

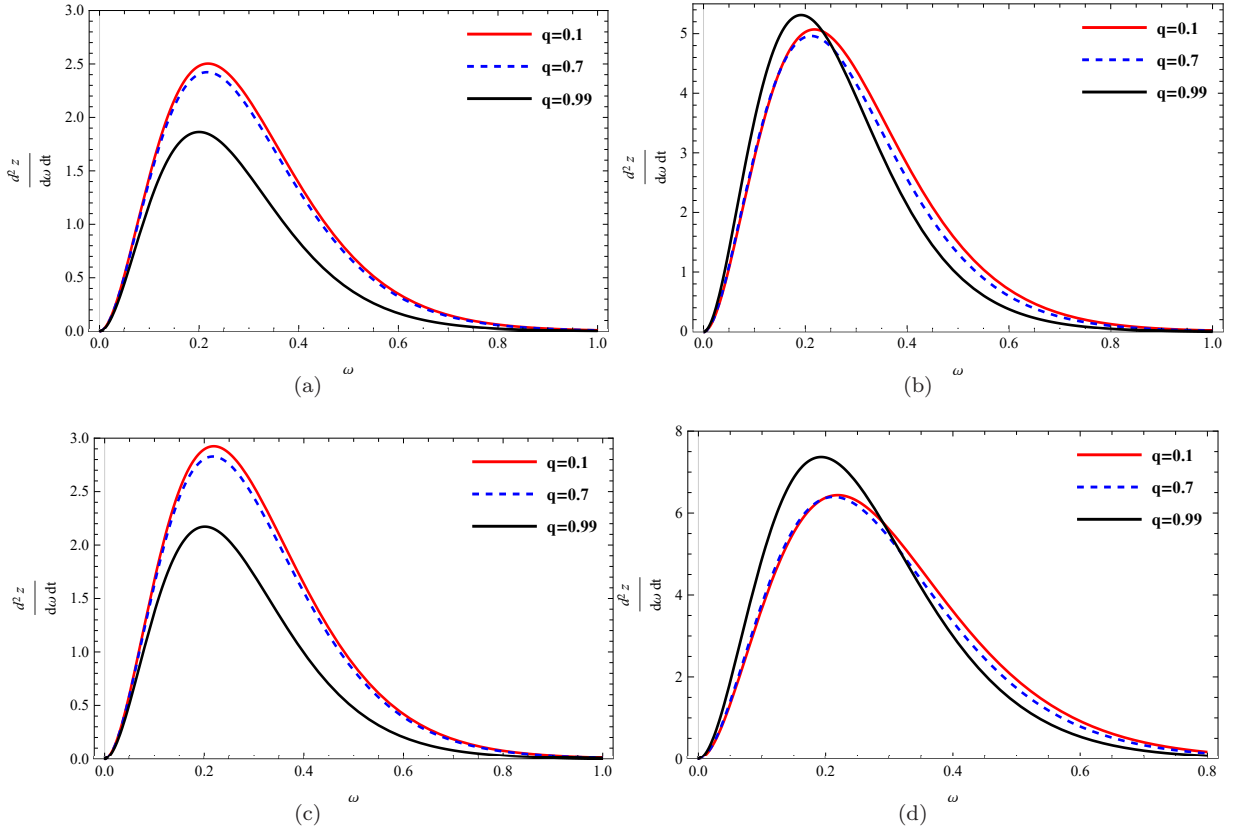


**Figure 8.** Variation of energy emission rate  $\frac{d^2Z(\omega)}{d\omega dt}$  with frequency  $\omega$  for changing charge  $q$  and changing photon sphere radius. In 8(a)  $k = 0, \Lambda = 0.018$ ; in 8(b)  $k = 0.2, \Lambda = 0.018$ ; in 8(c)  $k = 0, \Lambda = 0.0098$  and in 8(d)  $k = 0.2, \Lambda = 0.0098$ . For all cases  $M = 1$ .

using the Hamilton-Jacobi equation. Using the boundary condition of unstable circular orbit we determined the radius of the photon sphere and then by using the null geodesics we obtained the celestial coordinates  $(\alpha, \beta)$  which in turn gives the radius of the shadow. We make a table of the values of photon radius  $r_p$  and shadow radius  $R_s$  for different values of charge by computation and have done a graphical analysis for the black hole shadow in the celestial plane ( $\alpha$ - $\beta$  plane) for different values of charge. The plots declared that the size of the black hole shadow decreases for an increase in the value of the charge parameter  $q$  and for an increase in the value of cosmological constant. We found that shadow radius depends on the parameters like cosmological constant, charge and mass of the black hole. To check the dependency of the shadow radius on these parameters, we have made a graphical analysis and observed that shadow radius is a decreasing function of charge for fixed photon sphere radius. We then introduce a plasma medium in order to investigate the effect of refractive index ( $n$ ) on the unstable circular orbits of null-like

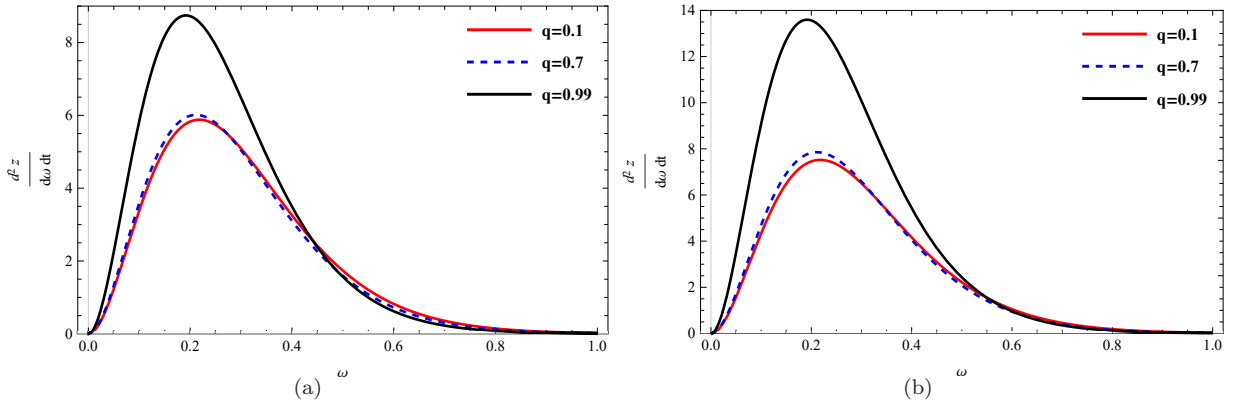


**Figure 9.** Variation of energy emission rate  $\frac{d^2Z(\omega)}{d\omega dt}$  with frequency  $\omega$  for changing charge  $q$  and changing photon sphere radius. In 9(a)  $k = 0.4$ ,  $\Lambda = 0.018$  and in 9(b)  $k = 0.4$ ,  $\Lambda = 0.0098$ . For all cases  $M = 1$ .

particles (photon). It is observed that shadow radius enlarges for an increase in plasma parameter  $k$  with changing photon sphere radius. The resulting shadow radius in the plasma medium has dependency on plasma parameter due to the refractive index of the plasma medium. We have done the graphical analyses for the plasma medium also, which reflects the effect of various parameters on shadow radius. Finally we studied the energy emission rate of the charged RN-AdS<sub>5</sub> black hole and have provided a graphical analysis of energy emission rate with respect to frequency. In the near future, similar to this study, by utilizing the mathematical optics, we will attempt to distinguish the differences between the BHs acquired from various theories.

### Data availability

Data sharing is not applicable to this article, as no data sets were generated or analyzed during the current study.

### Acknowledgement

The author is thankful to Dr. Sudhaker Upadhyay for various suggestions which developed the presentation of the paper.

### References

- [1] B. C. Bromley, F. Melia and S. Liu, *Astrophys.J.* 555, L83 (2001); A. deVries, *Phys. Unserer Zeit* 35, 128 (2004).

- [2] K. Hioki and K. I. Maeda, Phys. Rev. D 80, 024042 (2009).
- [3] Event Horizon Telescope Collaboration et al 2022 ApJL 930 L12.
- [4] J.M. Bardeen, in Black holes, in Proceeding of the Les Houches Summer School, Session 215239, edited by C. De Witt and B.S. De Witt and B.S. De Witt (Gordon and Breach, New York, 1973).
- [5] J.P. Luminet, Astron. Astrophys. 75, 228 (1979).
- [6] J.L. Synge, Mon. Not. R. Astron. Soc. 131, 463 (1966).
- [7] H. Falcke, F. Melia and E. Agol, Astrophys. J. 528, L13 (2000).
- [8] S. Chandrasekhar, The Mathematical Theory of Black Holes (Oxford University Press, New York, 1992).
- [9] V. Bozza, G. Scarpetta, Phys. Rev. D 76, 083008 (2007).
- [10] A. F. Zakharov, A. A. Nucita, F. DePaolis, and G. Ingrosso, New Astron. 10, 479 (2005); A. F. Zakharov, F. De Paolis, G. Ingrosso, and A. A. Nucita, Astron. Astrophys. 442, 795 (2005); F. De Paolis, G. Ingrosso, A.A. Nucita, A. Qadir, and A. F. Zakharov, Gen. Relativ. Gravit. 43, 977 (2011).
- [11] C. Bambi and K. Freese, Phys. Rev. D 79, 043002 (2009).
- [12] P. G. Nedkova, V. K. Tinchev, and S. S. Yazadjiev, Phys. Rev. D 88, 124019 (2013).
- [13] V. Bozza, Gen. Relativ. Gravit. 42, 2269 (2010).
- [14] H. C. Ohanian, Am. J. Phys. 55, 428 (1987); R. J. Nemiroff, Am. J. Phys. 61, 619 (1993); V. Bozza, S. Capozziello, G. Iovane, and G. Scarpetta, Gen. Relativ. Gravit. 33, 1535 (2001).
- [15] C. Darwin, Proc. Roy. Soc London A 249, 180 (1959).
- [16] A. Grenzebach, V. Perlick, C. Lmmerzahl, Phys. Rev. D 89, 124004 (2014).
- [17] V. Bozza, Phys. Rev. D 66, 103001 (2002).
- [18] Kraniotis, G.V. Gravitational lensing and frame dragging of light in the Kerr–Newman and the Kerr–Newman (anti) de Sitter black hole spacetimes. Gen Relativ Gravit 46, 1818 (2014).
- [19] M. Amir and S.G. Ghosh, Phys. Rev. D 94, 024054 (2016).
- [20] Z. Li and C. Bambi, JCAP 1401, 041 (2014).
- [21] A. Abdujabbarov, M. Amir, B. Ahmedov and S.G. Ghosh, Phys. Rev. D 93, 104004 (2016).
- [22] R. Takahashi, Publ. Astron. Soc. Jap. 57, 273 (2005).
- [23] A. Yumoto, D. Nitta, T. Chiba and N. Sugiyama, Phys. Rev. D 86, 103001 (2012).
- [24] L. Amarilla, E.F. Eiroa and G. Giribet, Phys. Rev. D 81, 124045 (2010).

- [25] L. Amarilla and E. F. Eiroa, Phys. Rev. D 85, 064019 (2012).
- [26] Ali Övgün and İzzet Sakallı 2020 Class. Quantum Grav. 37 225003.
- [27] Kimet Jusufi, Muhammed Amir, Md Sabir Ali, and Sunil D. Maharaj, Phys. Rev. D 102, 064020 (2020).
- [28] Eiroa, E.F., Sendra, C.M. Shadow cast by rotating braneworld black holes with a cosmological constant. Eur. Phys. J. C 78, 91 (2018).
- [29] G.T. Horowitz and T. Wiseman, arXiv:1107.5563.
- [30] H.S. Reall, Phys. Rev. D 68, 024024 (2003).
- [31] K. Hashimoto et al. Phys. Rev. Lett. 123, 031602 (2019).
- [32] Uma Papnoi, Farruh Atamurotov, Sushant G. Ghosh, and Bobomurat Ahmedo, Shadow of five-dimensional rotating Myers-Perry black hole, Phys. Rev. D 90, 024073 (2014).
- [33] Amir, M., Singh, B.P. & Ghosh, S.G. Shadows of rotating five-dimensional charged EMCS black holes. Eur. Phys. J. C 78, 399 (2018).
- [34] Guha, S., Bhattacharya, P. & Chakraborty, S. Particle motion in the field of a five-dimensional charged black hole. Astrophys Space Sci 341, 445–455 (2012).
- [35] D. Raine, E. Thomas: Black Holes An Introduction, 2nd edn. Imperial College Press, London (2005).
- [36] U. Papnoi et al. Phys. Rev. D 90, 024073 (2014).
- [37] A. Saha, S. Modumudi, S. Gangopadhyay, Gen. Rel. Grav. 50 (2018) 103.
- [38] J.L. Synge: Relativity: The General Theory. North Holland, Amsterdam (1960).
- [39] A. Rogers, Mon. Not. R. Astron. Soc. 451, 4536 (2015).
- [40] A. Saha, S. Modumudi, S. Gangopadhyay, Gen. Rel. Grav. 50 (2018) 103.
- [41] S.W. Wei, Y.X. Liu, J. Cosmol. Astropart. Phys. 11 (2013) 063.
- [42] Mashhoon, B. Scattering of Electromagnetic Radiation from a Black Hole. Phys. Rev. D 1973, 7, 2807. [CrossRef]
- [43] D. N. Page, Phys. Rev. D 13, 198 (1976).
- [44] Ali övgün, İzzet Sakallı, Joel Saavedra and Carlos Leiva, Modern Physics Letters A, Vol. 35, No. 20, 2050163 (2020).
- [45] Sudhaker Upadhyay, Nadeem-ul-islam, Prince A. Ganai, Journal of Holography Applications in Physics Volume 2, Issue 1, Winter 2022, 25-48.
- [46] Anish Das, Ashis Saha, Sunandan Gangopadhyay, Eur. Phys. J. C (2020) 80:180.
- [47] Y. Decanini, A. Folacci, B. Raffaelli, Class. Quant. Grav. 28, 175021 (2011).
- [48] B.P. Singh, S.G. Ghosh, Ann. Phys. 395 (2018) 127.

This figure "s1.png" is available in "png" format from:

<http://arxiv.org/ps/2207.10085v1>